dynamics

MDPI

Article

Baseline Electroencephalogram and Its Evolution after Activation of Dopaminergic System by Apomorphine in Middle-Aged 5XFAD Transgenic Mice, a Model of Alzheimer's Disease

Vasily Vorobyov [1,*], Alexander Deev [2], Zoya Oganesyan [3], Frank Sengpiel [4] and Aleksey A. Ustyugov [5]

[1] Institute of Cell Biophysics, Russian Academy of Sciences, 142290 Pushchino, Russia
[2] Institute of Theoretical and Experimental Biophysics, Russian Academy of Sciences, 142290 Pushchino, Russia
[3] International School "Medicine of the Future", Sechenov's First Moscow State Medical University, 119991 Moscow, Russia
[4] School of Biosciences and Neuroscience & Mental Health Research Institute, Museum Avenue, Cardiff University, Cardiff CF10 3AX, UK
[5] Institute of Physiologically Active Compounds, Russian Academy of Sciences, 142432 Chernogolovka, Russia
* Correspondence: vorobyovv2@gmail.com

Abstract: Aging and Alzheimer's disease (AD) are characterized by common pathological features associated with alterations in neuronal connections. These inevitably affect the functioning of specific brain areas and their interrelations, leading to questions about neuronal plasticity and the compensatory mechanisms associated with dopaminergic (DA) mediation. In this study on twelve-month-old freely moving 5XFAD-transgenic mice, serving as a model of AD, and their wild-type (WT) littermates, we analyze electroencephalograms (EEGs) from the motor cortex (MC), putamen (Pt) and the DA-producing ventral tegmental area (VTA) and substantia nigra (SN). Baseline EEGs in the transgenic mice were characterized by *delta 2* activity enhancements in VTA and *alpha* attenuation in VTA and SN. In contrast to WT mice, which lack differences in EEG from these brain areas, 5XFAD mice showed *theta–alpha* attenuation and *delta 2* and *beta 2* enhancements in EEG from both VTA and SN vs. MC. In 5XFAD mice, a DA mimetic, apomorphine, lowered (vs. saline) the *theta* oscillations in Pt, VTA and SN and enhanced *alpha* in MC, Pt, VTA and *beta 1* in all brain areas. These results and those obtained earlier in younger (six-month-old) mice suggest that the age-related characteristics of cerebral adaptive mechanisms affected by AD might be associated with modification of dopaminergic mediation in the mechanisms of intracerebral dynamic interrelations between different brain areas.

Keywords: Alzheimer's disease (AD); electroencephalogram (EEG); motor cortex; putamen; ventral tegmental area; substantia nigra

Citation: Vorobyov, V.; Deev, A.; Oganesyan, Z.; Sengpiel, F.; Ustyugov, A.A. Baseline Electroencephalogram and Its Evolution after Activation of Dopaminergic System by Apomorphine in Middle-Aged 5XFAD Transgenic Mice, a Model of Alzheimer's Disease. *Dynamics* **2022**, 2, 356–366. https://doi.org/10.3390/dynamics2040020

Academic Editor: Christos Volos

Received: 19 September 2022
Accepted: 10 October 2022
Published: 14 October 2022

1. Introduction

Alzheimer's disease (AD) and aging are characterized by relatively similar abnormalities in cognitive processing and inflammatory reactions, in neuronal connectivity and even in gene expression [1], which give rise to the question of synergistic mechanisms in the development of both processes. On the other hand, aging is well known as one of the major risk factors for AD. Comparative characterizations of young and aged brains in AD allow the differentiation of AD and aging mechanisms and the disclosure of their interrelations. In AD and aging, imbalances in the intra-/inter-neuronal circuits of different brain structures [2,3] (see for review [4,5]) have been shown to result in modification of oscillations in the affected networks [6,7]. This might be one of the critical targets for AD treatment [8] and/or for protection from age-dependent pathological changes in the brain. Oscillations of extracellular fields arising from synaptic transmembrane currents of neuronal populations are thought to be the source of the electroencephalogram (EEG) [9]. Its frequency compositions have been shown to correlate with AD pathology [10]. In

spite of evident dependence of brain processing on the interactions between neuronal groups [11], few studies of AD-associated cerebral mechanisms have been performed with simultaneous recordings of EEG from several brain areas [12–14]. In a rat "*beta*-amyloid" model of AD, the dopaminergic (DA) system involvement in the intracerebral network functioning has been shown [15]. On the other hand, DA signaling has been demonstrated to be involved in aging as well (for review [16]). In our previous study on relatively young (six-month-old) 5XFAD mice, EEGs from the motor cortex and DA-producing neuronal populations of ventral tegmental area (VTA) and substantia nigra (SN) were simultaneously recorded [17]. Baseline EEGs from VTA and SN showed *delta–theta* activity suppression and *beta* domination vs. those in wild-type (WT) littermates. Furthermore, while the EEGs from VTA and SN vs. the cortex in WT mice were characterized by enhanced activities in the *delta 2-alpha* range and suppressed in the *beta* band, these differences were significantly attenuated in the 5XFAD mice. Moreover, the EEG interrelations within and between the brain areas have been shown to be affected by a DA mimetic, apomorphine (APO).

This study was performed on middle-aged (twelve-month-old) 5XFAD and WT mice to compare the EEG data with those obtained on younger (six-month-old) mice used in similar experimental conditions in our previous study [17]. In the frequency spectra of EEGs recorded from different brain structures before and after a subcutaneous injection of APO, significant differences between (a) 5XFAD mice and their WT littermates and (b) middle-aged and young animals were demonstrated.

2. Materials and Methods

In this study, the middle-aged (12-month-old) male 5XFAD (Tg, $n = 9$) mice and wild-type littermates (nTg, $n = 7$) were used. The mice were obtained from Chernogolovka's Center for Collective Use of the Institute of Physiologically Active Compounds RAS (Russian Federation). The mice were reared in the standard conditions with food and water ad libitum. The study was performed in accordance with the Directive 2010/63/EU and approved by the local Institute Ethics Review Committee (protocol No 52, 18 September 2020).

2.1. Electrodes Implantation and EEG Recording

Each of the nine Tg and seven nTg mice (37.4 ± 1.4 g and 52.4 ± 2.9 g, respectively) was subcutaneously (s.c.) injected with tiletamine/zolazepam (25 mg/kg, Zoletil®, Virbac, Carros, France) and xylazine (2.5 mg/kg, Rometar®, Bioveta, Komenskйho, Czech Republic) mixture.

Recording electrodes were positioned in several brain areas: the left motor cortex (MC, AP: +1.1 mm; ML: ±1.5 mm; DV: −0.75 mm); the putamen (Pt; AP: +1.1 mm; ML: ±1.5 mm; DV: −2.75 mm); the left ventral tegmental area (VTA; AP: −3.1, ML: −0.4, DV: −4.5); and the right substantia nigra (SN; AP: −3.2, ML: +1.3, DV: −4.3) [18].

The electrodes were prepared from two varnish-insulated nichrome wires (100 μm in diameter) that were glued together with the tips free from insulation for 100 μm. The reference and ground electrodes (stainless steel wire, 0.4 mm in diameter) were stereotaxically positioned over the caudal part of the brain. After the electrodes were fixed to the skull, they were soldered to a mini-connector. For post-mortem evaluation of the electrode position, the brains were fixed in accordance with standard procedures (see for details [19]). Brain sections of an 8 μm thickness were mounted onto poly-L-lysine–coated slides for the stereological counting technique, as described previously [20]. One of five slides from each of eight series was stained with hematoxylin and eosin. Electrode positions in Pt and MC were visualized without staining, whereas for those in SN and VTA another slide was stained with antibodies against tyrosine hydroxylase (TH, mouse monoclonal antibody, clone TH-2, Sigma, diluted 1:1000) and glial fibrillary acidic protein (rabbit monoclonal antibody, Sigma G9269, diluted 1:1000) with fluorescent detection by use of Alexa Fluor 488 (Thermo A11029, diluted 1:1000) and Alexa Fluor 568 (Thermo A11011, diluted 1:1000) (see for details [21]). The borders of SN and VTA were outlined using the atlas of TH-positive cells distribution [22]. The slices with the most effective electrode positions and treated as

mentioned above were magnified and digitized for a fluorescence detection, followed by the preparation of high-quality photographs on a laser scanning confocal microscope LSM 880 (Carl Zeiss) for further illustration (see an example in Figure S1).

After three post-implantation days, each mouse was daily placed in an electrically shielded experimental cage and connected to a cable that was plugged into a digital amplifier. On day 8, the 30 min baseline EEG was recorded after 20–30 min of adaptation to the environment. Then, EEG was recorded for 60 min after a s.c. injection with saline or apomorphine (APO, 1.0 mg/kg, Sigma, Milan, Italy) (see for details [17]).

2.2. Computation of EEG Frequency Spectra

EEG signals were analyzed by using a home-prepared program based on a period-amplitude approach [23], which automatically "cleared" EEG from potentially abnormal features. EEG was analyzed in the range of 0.5–32-Hz and afterwards, in "classical" EEG bands from delta 1 to beta 2 (see for details [17]).

Initially, the EEG spectra obtained on 12-s epochs were averaged for 10 min intervals individually for each mouse and then throughout the 5XFAD and control groups separately. The averaged EEG spectra obtained after injections of saline (day 1) or APO (day 2), were normalized vs. baseline values and presented as a ratio of (APO—saline)/saline, in %, to evaluate the APO effects.

2.3. Statistics

For the comparison of EEG amplitudes in the "classical" frequency bands averaged for 10 min, one- or two-way ANOVAs were used when appropriate (STATISTICA 10 (StatSoft, Inc., Tulsa, OK, USA)). The threshold level of significance was chosen as $p < 0.05$.

3. Results

3.1. Baseline EEG

During EEG recordings, both 5XFAD mice and their littermates explored the experimental box, which was rarely interrupted by short sleep-like bouts.

In nTg and Tg mice, the raw baseline EEGs from all brain structures were characterized by slow waves (Figure 1A,B) and, consequently, by elevated *theta* values in the individual frequency spectra (Figure 1C–F).

The differences between the groups were relatively stable in the EEG spectra averaged over three consecutive 10 min intervals and readily visible in the spectral profiles that characterized the whole (30 min) baseline period (Figure 2).

In Tg vs. nTg mice, in the averaged spectra of the baseline EEG from VTA, *delta* activity was increased and *alpha* was decreased (Figure 3B,D; two-way ANOVA: $F_{1,42} = 6.8$ and 11.6, $p = 0.01$ and 0.001, respectively). In EEGs from SN, *delta* tended to be enhanced in the Tg group (Figure 3B), while *alpha* was significantly attenuated (Figure 3D; two-way ANOVA: $F_{1,42} = 6.5$, $p = 0.015$). In Tg mice, EEGs from VTA vs. MC were characterized by enhanced *delta 2* and *beta 2* (Figure 3B,F; two-way ANOVA: $F_{1,48} = 5.4$ and 6.1, $p = 0.025$ and 0.017, respectively) and attenuated *theta* and *alpha* (Figure 3C,D; two-way ANOVA: $F_{1,48} = 7.0$ and 9.5, $p = 0.011$ and 0.003, respectively). In EEGs from SN vs. MC in Tg mice, *theta* and *alpha* activities were reduced (Figure 3C,D; two-way ANOVA: $F_{1,48} = 9.9$ and 6.3, $p = 0.003$ and 0.001, respectively), whereas *beta 2* activity was enhanced (Figure 3F; two-way ANOVA: $F_{1,48} = 11.6$, $p = 0.016$). In nTg mice, no differences between baseline EEGs from the brain structures were observed (Figure 3, open bars).

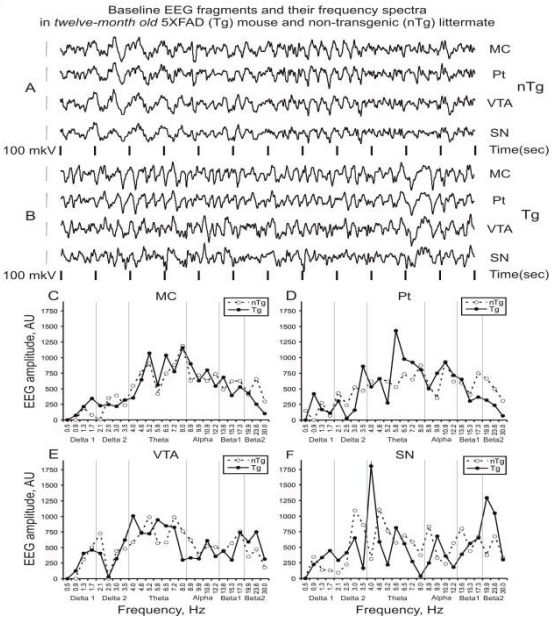

Figure 1. Differences in raw baseline EEGs in control (nTg) and 5XFAD (Tg) mice (**A**,**B**) and in their frequency compositions in different brain structures ((**C**)—motor cortex, MC; (**D**)—putamen, Pt; (**E**)—ventral tegmental area, VTA; (**F**)—substantia nigra, SN). In (**C**–**F**), abscissa is a frequency sub-band, in hertz (vertical grey lines denote the "classical" EEG bands); the ordinate is a normalized EEG amplitude, in arbitrary units.

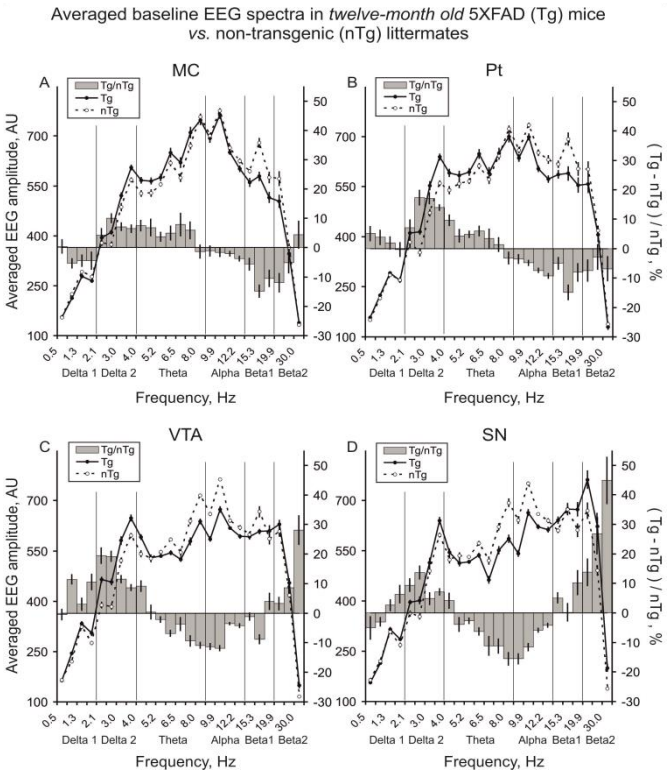

Figure 2. Differences in frequency compositions of baseline EEGs recorded from different brain structures ((**A**)—motor cortex, MC; (**B**)—putamen, Pt; (**C**)—ventral tegmental area, VTA; (**D**)—substantia nigra, SN) in 5XFAD (Tg, $n = 9$) and control (nTg, $n = 7$) mice. Abscissa is a frequency sub-band, in hertz (vertical grey lines denote the "classical" EEG bands); the ordinates are normalized EEG amplitudes, in arbitrary units (left), and their ratio of (Tg–nTg)/nTg, in %. Error bars show ± 1 SEM.

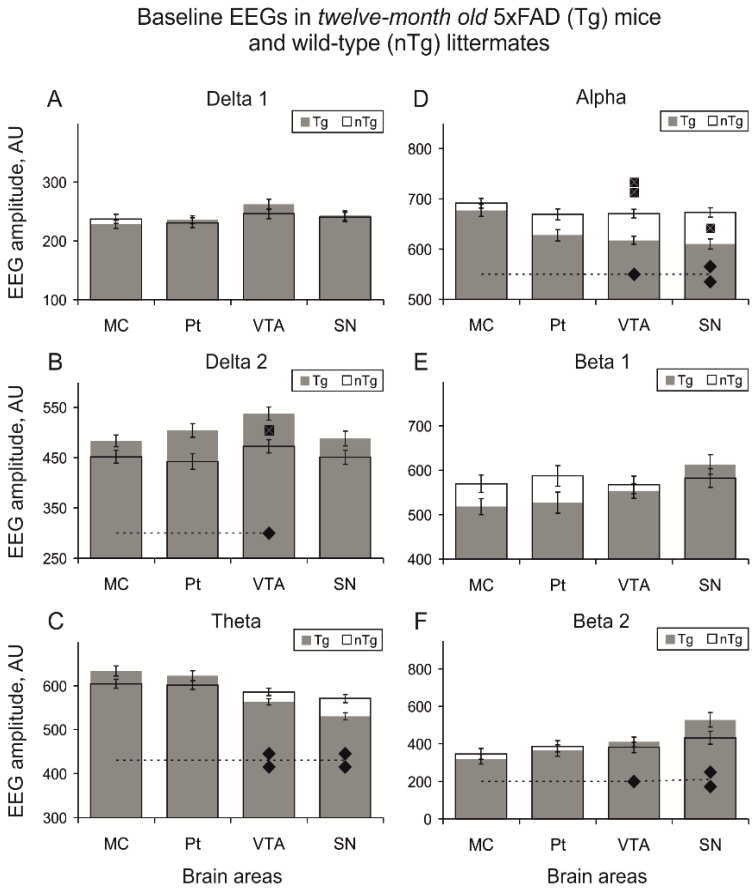

Figure 3. Relations between "classical" frequency bands values (**A**–**F**) averaged for 30 min of continuous baseline EEG recordings from MC, Pt, SN, and VTA in twelve-month-old nTg (n = 7) and Tg (n = 9) mice (open and filled bars, respectively). Horizontal axis denotes brain areas; vertical axis is the normalized sum of EEG amplitudes in "classical" frequency bands for corresponding brain area. Error bars show ±1 SEM.; filled diamonds and quadrates denote significant differences (two-way ANOVA) between selected brain area and MC, and between Tg and nTg groups, respectively ($p < 0.05$ and $p < 0.01$, one and two symbols, respectively).

3.2. Apomorphine Effects

APO provoked very similar reactions in mice from both groups: initial 1.5–2 min freezing, 20–25 min tail erection and 30–40 min licking of the box's floor and walls. Very rare and short sleep-like bouts occurred at variable times after APO injection.

In Tg mice, APO produced initial *delta 2* suppression with incremental recovery in MC, Pt and VTA (Figure 4b (A–C); one-way ANOVA: $F_{5,48}$ = 3.8, 9.0 and 5.0, $p < 0.01$, 0.001 and 0.001, respectively), whereas in nTg mice, similar trends in *delta 2* evolution did not reach significance. After APO injection, observed inverse changes in *alpha* vs. *delta 2* profiles did not reach significance in mice from either group (c.f., Figure 4b,d). In Tg vs. nTg mice, APO affected EEGs from all brain areas but MC: it significantly suppressed *theta* in Pt, VTA and SN (Figure 4c (B–D); two-way ANOVA: $F_{1,84}$ = 12, 10 and 20.3, $p < 0.001$, 0.01 and 0.001, respectively) and amplified *beta 1* in all brain areas (Figure 4e; two-way ANOVA: $F_{1,84}$ = 9.8, 22.5, 19.7 and 16.5, $p < 0.01$, 0.001, 0.001 and 0.001, for MC, Pt, VTA and SN, respectively).

In the *beta 2* band, only a significant Tg vs. nTg difference was observed in EEGs from Pt (Figure 4f (B); two-way ANOVA: $F_{1,84}$ = 7.1, $p < 0.01$). After saline injection, no evident EEG differences between Tg and nTg mice were observed in any brain area (Figure S2).

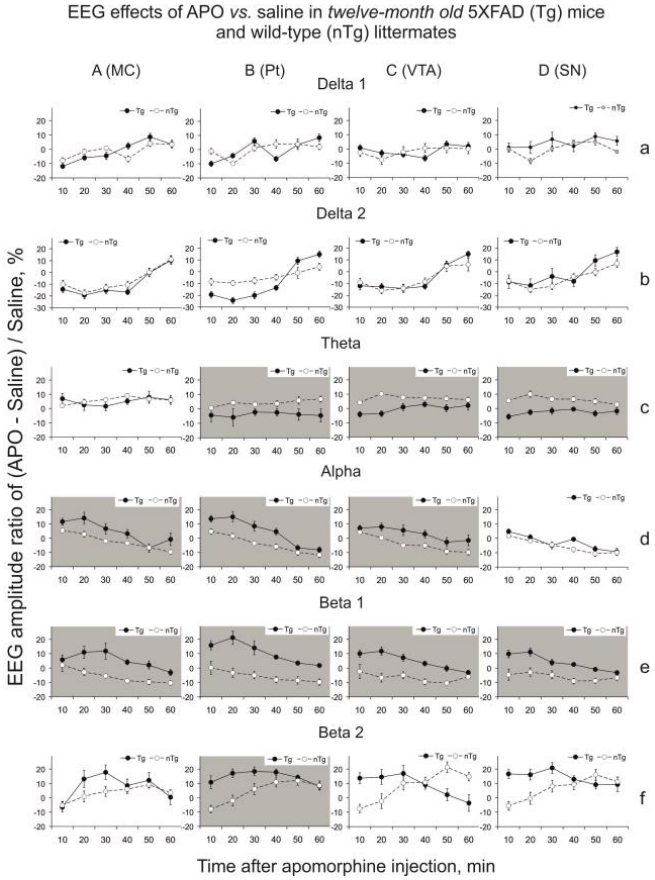

Figure 4. Evolution of APO (1.0 mg/kg, s.c.) vs. saline effects in "classical" frequency bands (**a**–**f**) of EEG spectra in MC, Pt, VTA and SN (**A**–**D**) in twelve-month-old nTg (n = 7) and Tg (n = 9) mice (dashed and solid lines, respectively). Abscissa shows time after injection; ordinate is a ratio of EEG amplitudes in each group calculated as (APO—saline)/saline, in %. Grey-colored plate denotes a significant difference (two-way ANOVA) between the groups. Error bars show ±1 SEM.

4. Discussion

4.1. Baseline EEG

In twelve-month-old transgenic 5XFAD (Tg) mice vs. their non-transgenic (nTg) littermates, we have shown both slow-wave (*delta 2*) enhancement in baseline EEGs from the ventral tegmental area (VTA) with a similar trend in the substantia nigra (SN), and significant *alpha* activity attenuation in these brain areas (Figure 3B,D, respectively). In contrast to nTg mice, which were characterized by relatively similar levels of EEG activity in each of the "classical" frequency bands in all structures (Figure 3, open bars), in Tg mice, an enhancement of the *delta 2* and *beta 2* (Figure 3B,F, filled bars, respectively) and attenuation of the *theta* and *alpha* (Figure 3C,D, gray bars, respectively) in VTA and SN vs. those in MC were observed.

Together, the profiles of the frequency spectra of EEGs from MC, VTA and SN in twelve-month-old Tg mice and their nTg littermates were evidently different from those in six-month-old genetically-matched mice (here and below, the EEG data obtained from six-month-old ("younger") mice are taken from our previous study [17]). EEG spectra in older mice were characterized by *theta* activity dominating in all brain structures, whereas in younger mice, there was a peak in *beta 2* activity in MC and HPC but nearly equal strength of *delta 2*—*beta 2* oscillations in EEGs from VTA and SN. Moreover, whereas in the Tg vs. nTg groups, EEGs from VTA and SN in older mice were characterized by *delta 2* enhancement and *alpha* attenuation, in younger mice, the *theta* activity was attenuated, and *beta* was enhanced. In general, significant EEG differences present in younger nTg mice between DA-containing areas (VTA and SN), and MC were practically eliminated in Tg

mice. Interestingly, in younger mice, the differences in *alpha* activity between the brain areas were insensitive to AD-associated pathology. In older nTg mice, EEG oscillations in the "classical" bands were of similar amplitude in all brain areas, whereas in Tg littermates, evident band-dependent specificity of EEG changes was observed between DA-containing areas and MC (Figure 3B–D,F, filled bars). This rearrangement of neuronal networks might be explained by an interaction of brain adaptive age-associated mechanisms [24] and AD-produced modifications in their functioning [25].

Substantial *theta* enhancement in EEG from MC in older vs. younger nTg mice is in line with what has been observed in the cortex of aging C57BL/6 mice [26]. In younger Tg vs. nTg mice, the *delta* and *alpha* enhancement in EEG from, a hallmark of "non-REM" sleep [27], was accompanied by significant suppression of *beta 2* oscillations in Tg mice. The transformations in EEG from MC in Tg mice seem to be connected with disturbed functioning of the affected oscillatory circuits that may be considered as adaptive remodeling in response to AD-associated neurotoxicity and neurodegeneration observed in 5XFAD mice [28]. Indeed, substantial *theta* activity in older vs. younger mice is more likely linked with specific remodeling mechanisms that are activated to similar extents in Tg and nTg mice by aging alone or in combination with AD. Furthermore, these mechanisms appear to be specific, as their functioning is unlikely to be affected by changes in behavior, which have been shown to be characterized by opposite trends in their regulation in aging 5XFAD and non-transgenic mice (see [29,30], respectively).

It should be noted, that in older mice, the most significant Tg vs. nTg differences were observed in baseline EEGs from VTA and SN and characterized by attenuated *alpha* oscillations, whereas in younger Tg mice, attenuated *theta* and enhanced *beta 1* and *beta 2* activities have been shown in our previous study. Interestingly, the EEG changes in VTA and SN in younger 5XFAD mice correlated with significant losses of DA-containing neurons in these brain areas. The phenomenon is supposed to be universal for AD and other neurodegenerative disorders [31]. Thus, the EEG approach allows indirect characterization of DA-containing areas and their involvement in various functional networks in normal and pathological conditions. The *theta* and *beta* activities affected by AD in younger mice seem to be associated with so-called "tonic" (*delta-theta*) and "bursting" (*beta*) neuronal activities observed in the DA-accumulating mid-brain [32,33]. Thus, *theta* attenuation and *beta* enhancement might be correlated with a suppression of tonic firing and elevation of bursting in VTA and SN in younger Tg mice, which is possibly associated with significant shrinkage of DA-producing neuronal populations in these brain areas [17]. In contrast to the EEG changes observed in younger Tg vs. nTg mice, in older Tg mice, only *alpha* activity was lowered (Figure 3D). Thus, whereas interconnections between SN and VTA [34] in younger mice are seemingly tuned to *alpha* synchronization in these areas in both Tg and nTg mice, in older mice, evident attenuation of *alpha* activity was observed in Tg mice only. This is thought to be linked with age-associated changes in specific compensatory mechanisms activated by neuronal deficit in SN and VTA in younger Tg mice [35], in contrast to the relative stability of DA-containing neuronal populations observed in nTg mice as old as eight to twelve months [36] and older [37]. The bursts in VTA have been shown to be initiated by MC activation [38], which, in turn, effectively stimulates DA release in the cortex [39,40], thereby supporting a MC-VTA network functioning. In Tg mice, DA depletion, which is evoked by a loss of DA-containing neurons, is well known to initiate compensatory sensitization of DA synapses in the cortex [41]. These explain the evident attenuation of tonic (*theta*) and amplification of bursting (*beta*) activities in VTA and SN in young Tg vs. nTg mice as a compensatory/adaptive response of the affected networks at a systemic level. However, the AD-associated sensitization of DA receptors was ineffective for further corrections of neuronal network activity in older Tg vs. nTg mice (see Figure 3E,F). The source of the age-dependent changes in the compensatory capability of systemic adaptive mechanisms might be associated, in particular, with the development of senescent processes in the brain [42] that need to be analyzed in further studies.

4.2. Apomorphine Effects

In twelve-month-old transgenic 5XFAD (Tg) mice vs. their non-transgenic (nTg) littermates, APO (*vs.* saline) lowered *theta* activity in EEGs from Pt, VTA and SN (Figure 4c (B–D), respectively) and enhanced both *alpha* in MC, Pt and VTA (Figure 4c (A–C), respectively) and *beta 1* in all brain regions (Figure 4e). The APO effects in *beta 1* band were evidently more powerfully expressed in older than in younger Tg mice (see 17]). This means that DA receptor supersensitization, which is linked with DA neuron loss in VTA and SN [43], seems to dominate over systemic (network) compensatory mechanisms supporting DA mediation in old and young Tg mice. Significant APO-produced enhancement of *beta 1* ("bursting" [32]) activity in both VTA and SN in Tg mice (Figure 4e (C,D), solid lines) might be produced by an enhanced feed-back stimulating influence activated by APO cortical neurons on the midbrain DA areas [39], in order to support their bursting activities, which are suppressed by APO in nTg littermates (Figure 4e (C,D), dashed lines). On the other hand, the APO-produced suppression of *delta 2* activity in EEGs from VTA and SN (Figure 4b (C,D), respectively) in both groups of mice match for relatively normal tonic firing of the DA neurons [33], which was also observed in younger mice. However, characteristic APO-associated differences in cortical *delta 2* in younger Tg vs. nTg mice, which were eliminated in older mice, seem to underline a role of age-related modifications in cortical DA receptor sensitivity that is associated with the loss of DA neurons in the brain of control littermates as well [37]. Furthermore, the identical profiles of cortical *delta 2* evolution after APO injection in older Tg and nTg mice (Figure 4b (A)) appear to be in line with the suggestion of non-additive mechanisms for EEG slow waves in aging and AD-associated pathology in humans [44]. The APO-produced suppression of *theta* oscillations in Pt, VTA and SN in older Tg vs. nTg mice (Figure 4c (B–D), respectively) might be associated with a compensatory desensitization of both pre- and post-synaptic DA receptors [41] produced by increased DA concentration in the synaptic clefts, which, in turn, is caused by a DA transporter deficit, characteristic of the 5XFAD model of AD [17]. Together, the tonic (*delta*) neuronal activities in the DA-producing areas [32,33], which are suppressed to comparable extents in Tg and nTg mice of both ages, underline a stability of the sensitivities of DA receptors involved in the functioning of neuronal circuits that generate *delta 2* EEG activity in mice from these groups. In contrast, significantly enhanced bursting (*beta 1*) activities in EEG from VTA and SN in older Tg mice (Figure 4e (C,D), respectively) and similar trends in younger Tg vs. nTg mice demonstrate the age-related disturbances in a balanced interaction between compensatory network functions and enhanced DA receptor sensitivities in AD. In older Tg mice, the supersensitization of DA receptors dominates over the activity of the VTA and SN networks, demonstrating limitations in their compensatory capabilities.

5. Conclusions

EEG monitoring of age-dependent modifications in the dynamic characteristics of "local" and "systemic" compensatory mechanisms (at the levels of receptors and networks, respectively) allows both the prediction of possible changes in the functioning of aging brains and the development of novel approaches for AD therapy aimed at strengthening compensatory mechanisms of network plasticity.

Supplementary Materials: The following supporting information can be downloaded at: https://www.mdpi.com/article/10.3390/dynamics2040020/s1, Figure S1: Coronal section of the mouse brain (**A**) and (**B**) at the level of VTA, and SN with verification of dopaminergic neurons and the nuclei (**C**) and (**D**) by TH (green signal) and DAPI. Horizontal scale bars denote 500 мkm; Figure S2: Saline produced no substantial changes in "classical" frequency bands (**a**–**f**) of EEG from different brain structures (**A**–**D**): the motor cortex (MC), putamen (Pt), ventral tegmental area (VTA) and substantia nigra (SN) in twelve-month-old 5XFAD mice (Tg, $n = 9$) and non-transgenic littermates (nTg, $n = 7$) (solid and dashed lines, respectively). Abscissa shows time after injection, marked in 10 min intervals; ordinate is summed absolute values of EEG amplitudes (in arbitrary units) in each of "classical" frequency bands, normalized to sum of all amplitudes of baseline EEGs recorded from corresponding

brain area. No significant time-dependent differences in and between Tg and nTg mice (one- and two-way ANOVA, when appropriate). Error bars show ±1 SEM.

Author Contributions: Conceptualization, methodology, investigation and original draft preparation, V.V.; software, A.D.; investigation and formal analysis, Z.O.; review and editing, F.S.; resources, project administration and funding acquisition, A.A.U. All authors have read and agreed to the published version of the manuscript.

Funding: This research received no external funding.

Institutional Review Board Statement: The animal study protocol was approved by by the local Institute Ethics Review Committee (protocol No 52, 18 September 2020).

Informed Consent Statement: Not applicable.

Data Availability Statement: The data are contained within the article and supplementary materials.

Acknowledgments: This work was supported by Grant RSF 18-15-00392. Animals were supported by the budget of the IPAC RAS State Targets topic # 0090-2019-0005.

Conflicts of Interest: The authors declare no conflict of interest.

References

1. Peng, S.; Zeng, L.; Haure-Mirande, J.V.; Wang, M.; Huffman, D.M.; Haroutunian, V.; Ehrlich, M.E.; Zhang, B.; Tu, Z. Transcriptomic Changes Highly Similar to Alzheimer's Disease Are Observed in a Subpopulation of Individuals during Normal Brain Aging. *Front. Aging Neurosci.* **2021**, *13*, 711524. [CrossRef] [PubMed]
2. Wang, P.; Zhou, B.; Yao, H.; Zhan, Y.; Zhang, Z.; Cui, Y.; Xu, K.; Ma, J.; Wang, L.; An, N.; et al. Aberrant intra- and inter-network connectivity architectures in Alzheimer's disease and mild cognitive impairment. *Sci. Rep.* **2015**, *5*, 14824. [CrossRef] [PubMed]
3. Wu, Z.; Gao, Y.; Potter, T.; Benoit, J.; Shen, J.; Schulz, P.E.; Zhang, Y. The Alzheimer's Disease Neuroimaging Initiative Interactions between Aging and Alzheimer's Disease on Structural Brain Networks. *Front. Aging Neurosci.* **2021**, *13*, 639795. [CrossRef]
4. Babiloni, C.; Blinowska, K.; Bonanni, L.; Cichocki, A.; De Haan, W.; Del Percio, C.; Dubois, B.; Escudero, J.; Fernández, A.; Frisoni, G.; et al. What electrophysiology tells us about Alzheimer's disease: A window into the synchronization and connectivity of brain neurons. *Neurobiol. Aging* **2020**, *85*, 58–73. [CrossRef] [PubMed]
5. Watanabe, H.; Bagarinao, E.; Maesawa, S.; Hara, K.; Kawabata, K.; Ogura, A.; Ohdake, R.; Shima, S.; Mizutani, Y.; Ueda, A.; et al. Characteristics of Neural Network Changes in Normal Aging and Early Dementia. *Front. Aging Neurosci.* **2021**, *13*, 747359. [CrossRef] [PubMed]
6. Nimmrich, V.; Draguhn, A.; Axmacher, N. Neuronal Network Oscillations in Neurodegenerative Diseases. *Neuromolecular Med.* **2015**, *17*, 270–284. [CrossRef] [PubMed]
7. Palop, J.J.; Mucke, L. Network abnormalities and interneuron dysfunction in Alzheimer disease. *Nat. Rev. Neurosci.* **2016**, *17*, 777–792. [CrossRef] [PubMed]
8. Canter, R.G.; Penney, J.; Tsai, L.H. The road to restoring neural circuits for the treatment of Alzheimer's disease. *Nature* **2016**, *539*, 187–196. [CrossRef] [PubMed]
9. Buzsáki, G.; Anastassiou, C.A.; Koch, C. The origin of extracellular fields and currents—EEG, ECoG, LFP and spikes. *Nat. Rev. Neurosci.* **2012**, *13*, 407–420. [CrossRef]
10. Koenig, T.; Prichep, L.; Dierks, T.; Hubl, D.; Wahlund, L.O.; John, E.R.; Jelic, V. Decreased EEG synchronization in Alzheimer's disease and mild cognitive impairment. *Neurobiol. Aging* **2005**, *26*, 165–171. [CrossRef] [PubMed]
11. Womelsdorf, T.; Schoffelen, J.M.; Oostenveld, R.; Singer, W.; Desimone, R.; Engel, A.K.; Fries, P. Modulation of neuronal interactions through neuronal synchronization. *Science* **2007**, *316*, 1609–1612. [CrossRef]
12. Crouzin, N.; Baranger, K.; Cavalier, M.; Marchalant, Y.; Cohen-Solal, C.; Roman, F.S.; Khrestchatisky, M.; Rivera, S.; Féron, F.; Vignes, M. Area-specific alterations of synaptic plasticity in the 5XFAD mouse model of Alzheimer's disease: Dissociation between somatosensory cortex and hippocampus. *PLoS ONE* **2013**, *8*, e74667. [CrossRef] [PubMed]
13. Schneider, F.; Baldauf, K.; Wetzel, W.; Reymann, K.G. Behavioral and EEG changes in male 5XFAD mice. *Physiol. Behav.* **2014**, *135*, 25–33. [CrossRef]
14. Siwek, M.E.; Müller, R.; Henseler, C.; Trog, A.; Lundt, A.; Wormuth, C.; Broich, K.; Ehninger, D.; Weiergräber, M.; Papazoglou, A. Altered *theta* oscillations and aberrant cortical excitatory activity in the 5XFAD model of Alzheimer's disease. *Neural Plast.* **2015**, *2015*, 781731. [CrossRef] [PubMed]
15. Vorobyov, V.; Kaptsov, V.; Gordon, R.; Makarova, E.; Podolski, I.; Sengpiel, F. Neuroprotective effects of hydrated fullerene C60, cortical and hippocampal EEG interplay in an amyloid-infused rat model of Alzheimer's disease. *J. Alzheimers Dis.* **2015**, *45*, 217–233. [CrossRef]
16. Gasiorowska, A.; Wydrych, M.; Drapich, P.; Zadrozny, M.; Steczkowska, M.; Niewiadomski, W.; Niewiadomska, G. The Biology and Pathobiology of Glutamatergic, Cholinergic, and Dopaminergic Signaling in the Aging Brain. *Front. Aging Neurosci.* **2021**, *13*, 654931. [CrossRef]

17. Vorobyov, V.; Bakharev, B.; Medvinskaya, N.; Nesterova, I.; Samokhin, A.; Deev, A.; Tatarnikova, O.; Ustyugov, A.A.; Sengpiel, F.; Bobkova, N. Loss of Midbrain Dopamine Neurons and Altered Apomorphine EEG Effects in the 5XFAD Mouse Model of Alzheimer's Disease. *J. Alzheimers Dis.* **2019**, *70*, 241–256. [CrossRef] [PubMed]
18. Franklin, K.B.J.; Paxinos, G. *The Mouse Brain in Stereotaxic Coordinates*, 3rd ed.; Academic Press: New York, NY, USA, 2007.
19. Al-Wandi, A.; Ninkina, N.; Millership, S.; Williamson, S.J.; Jones, P.A.; Buchman, V.L. Absence of *alpha*-synuclein affects dopamine metabolism and synaptic markers in the striatum of aging mice. *Neurobiol. Aging* **2010**, *31*, 796–804. [CrossRef] [PubMed]
20. Connor-Robson, N.; Peters, O.M.; Millership, S.; Ninkina, N.; Buchman, V.L. Combinational losses of synucleins reveal their differential requirements for compensating age-dependent alterations in motor behavior and dopamine metabolism. *Neurobiol. Aging* **2016**, *46*, 107–112. [CrossRef] [PubMed]
21. Goloborshcheva, V.V.; Chaprov, K.D.; Teterina, E.V.; Ovchinnikov, R.; Buchman, V.L. Reduced complement of dopaminergic neurons in the substantia nigra pars compacta of mice with a constitutive "low footprint" genetic knockout of *alpha*-synuclein. *Mol. Brain* **2020**, *13*, 75. [CrossRef] [PubMed]
22. Hökfelt, T.; Martensson, R.; Björklund, A.; Kheinau, S.; Goldstein, M. *Handbook of Chemical Neuroanatomy*; Björklund, A., Hökfelt, T., Eds.; Elsevier Science B.V: Amsterdam, The Netherlands, 1984; Volume 2, pp. 277–379.
23. Gal'chenko, A.A.; Vorobyov, V.V. Analysis of electroencephalograms using a modified amplitude-interval algorithm. *Neurosci. Behav. Physiol.* **1999**, *29*, 157–160. [CrossRef] [PubMed]
24. Aron, L.; Zullo, J.; Yankner, B.A. The adaptive aging brain. *Curr. Opin. Neurobiol.* **2021**, *72*, 91–100. [CrossRef] [PubMed]
25. Tsai, L.H.; Madabhushi, R. Alzheimer's disease: A protective factor for the ageing brain. *Nature* **2014**, *507*, 439–440. [CrossRef] [PubMed]
26. Del Percio, C.; Drinkenburg, W.; Lopez, S.; Infarinato, F.; Bastlund, J.F.; Laursen, B.; Pedersen, J.T.; Christensen, D.Z.; Forloni, G.; Frasca, A.; et al. On-going electroencephalographic rhythms related to cortical arousal in wild-type mice: The effect of aging. *Neurobiol. Aging* **2017**, *49*, 20–30. [CrossRef]
27. Vyazovskiy, V.V.; Achermann, P.; Borbély, A.A.; Tobler, I. The dynamics of spindles and EEG slow-wave activity in NREM sleep in mice. *Arch. Ital. Biol.* **2004**, *142*, 511–523. [PubMed]
28. Oakley, H.; Cole, S.L.; Logan, S.; Maus, E.; Shao, P.; Craft, J.; Guillozet-Bongaarts, A.; Ohno, M.; Disterhoft, J.; Van Eldik, L.; et al. Intraneuronal β-amyloid aggregates, neurodegeneration, and neuron loss in transgenic mice with five familial Alzheimer's disease mutations: Potential factors in amyloid plaque formation. *J. Neurosci.* **2006**, *26*, 10129–10140. [CrossRef]
29. Oblak, A.L.; Lin, P.B.; Kotredes, K.P.; Pandey, R.S.; Garceau, D.; Williams, H.M.; Uyar, A.; O'Rourke, R.; O'Rourke, S.; Ingraham, C.; et al. Comprehensive Evaluation of the 5XFAD Mouse Model for Preclinical Testing Applications: A MODEL-AD Study. *Front. Aging Neurosci.* **2021**, *13*, 713726. [CrossRef] [PubMed]
30. Yanai, S.; Endo, S. Functional Aging in Male C57BL/6J Mice Across the Life-Span: A Systematic Behavioral Analysis of Motor, Emotional, and Memory Function to Define an Aging Phenotype. *Front. Aging Neurosci.* **2021**, *13*, 697621. [CrossRef] [PubMed]
31. Krashia, P.; Nobili, A.; D'Amelio, M. Unifying Hypothesis of Dopamine Neuron Loss in Neurodegenerative Diseases: Focusing on Alzheimer's Disease. *Front. Mol. Neurosci.* **2019**, *12*, 123. [CrossRef]
32. Paladini, C.A.; Roeper, J. Generating bursts (and pauses) in the dopamine midbrain neurons. *Neuroscience* **2014**, *282*, 109–121. [CrossRef] [PubMed]
33. Hage, T.A.; Khaliq, Z.M. Tonic firing rate controls dendritic Ca^{2+} signaling and synaptic gain in substantia nigra dopamine neurons. *J. Neurosc.i* **2015**, *35*, 5823–5836. [CrossRef] [PubMed]
34. Ferreira, J.G.; Del-Fava, F.; Hasue, R.H.; Shammah-Lagnado, S.J. Organization of ventral tegmental area projections to the ventral tegmental area-nigral complex in the rat. *Neuroscience* **2008**, *153*, 196–213. [CrossRef] [PubMed]
35. Golden, J.P.; Demaro, J.A., III; Knoten, A.; Hoshi, M.; Pehek, E.; Johnson, E.M., Jr.; Gereau, R.W., IV; Jain, S. Dopamine-dependent compensation maintains motor behavior in mice with developmental ablation of dopaminergic neurons. *J. Neurosci.* **2013**, *33*, 17095–17107. [CrossRef] [PubMed]
36. Osterburg, H.H.; Donahue, H.G.; Severson, J.A.; Finch, C.E. Catecholamine levels and turnover during aging in brain regions of male C57BL/6J mice. *Brain Res.* **1981**, *224*, 337–352. [CrossRef]
37. Noda, S.; Sato, S.; Fukuda, T.; Tada, N.; Hattori, N. Aging-related motor function and dopaminergic neuronal loss in C57BL/6 mice. *Mol. Brain* **2020**, *13*, 46. [CrossRef]
38. Tong, Z.Y.; Overton, P.G.; Clark, D. Antagonism of NMDA receptors but not AMPA/kainate receptors blocks bursting in dopaminergic neurons induced by electrical stimulation of the prefrontal cortex. *J. Neural Transm.* **1996**, *103*, 889–904. [CrossRef]
39. Au-Young, S.M.; Shen, H.; Yang, C.R. Medial prefrontal cortical output neurons to the ventral tegmental area (VTA) and their responses to burst-patterned stimulation of the VTA: Neuroanatomical and in vivo electrophysiological analyses. *Synapse* **1999**, *34*, 245–255. [CrossRef]
40. Sesack, S.R.; Grace, A.A. Cortico-basal ganglia reward network: Microcircuitry. *Neuropsychopharmacology* **2010**, *35*, 27–47. [CrossRef]
41. Lohr, K.M.; Masoud, S.T.; Salahpour, A.; Miller, G.W. Membrane transporters as mediators of synaptic dopamine dynamics: Implications for disease. *Eur. J. Neurosci.* **2017**, *45*, 20–33. [CrossRef]
42. Nekrasov, P.V.; Vorobyov, V.V. Dopaminergic mediation in the brain aging and neurodegenerative diseases: A role of senescent cells. *Neural Regen. Res.* **2018**, *13*, 649–650. [CrossRef]

43. Kostrzewa, R.M.; Kostrzewa, J.P.; Brown, R.W.; Nowak, P.; Brus, R. Dopamine receptor supersensitivity: Development, mechanisms, presentation, and clinical applicability. *Neurotox. Res.* **2008**, *14*, 121–128. [CrossRef] [PubMed]
44. Prestia, A.; Baglieri, A.; Pievani, M.; Bonetti, M.; Rasser, P.E.; Thompson, P.M.; Marino, S.; Bramanti, P.; Frisoni, G.B. The in vivo topography of cortical changes in healthy aging and prodromal Alzheimer's disease. *Figure Clin. Neurophysiol.* **2013**, *62*, 67–80.